Fibers and Polymers 2020, Vol.21, No.4, 810-820
DOI 10.1007/s12221-020-8630-8

ISSN 1229-9197 (print version)
ISSN 1875-0052 (electronic version)

Removal of Methylene Blue in Aqueous Solution by Economic Adsorbent Derived from Apricot Stone Activated Carbon

Moussa Abbas[1]* and Mohamed Trari[2]

[1]*Laboratory of Soft Technologies and Biodiversity (LTDVPMBB), Chemical Department, Sciences Faculty, University M'hamed Bougara of Boumerdes, Boumerdes 35000, Algeria*
[2]*Laboratory of Storage and Valorization of Renewable Energies (LSVRE), Faculty of Chemistry, USTHB, BP 32-16111 El-Alia Alger 16000, Algeria*

(Received July 16, 2018; Revised August 17, 2019; Accepted September 23, 2019)

Abstract: Quantitative adsorption kinetic and equilibrium parameters for methylene blue (MB) used in the textile industry from aqueous solutions were reported in this study using pH_{PZC} and UV-visible absorption spectroscopy. The effects of adsorbent dosage (1-10 g/*l*), agitation speed (100-1200 rpm), particule size (63 μm to 2 mm), initial dye concentration (4-15 mg/*l*), contact time, pH (2-14), and temperature (298-338 K) were determined to find the optimal conditions for adsorption. The FTIR spectroscopy is used to get information on interactions between the adsorbent and MB. The mechanism of adsorption of MB dyeing onto Apricot Stone Activated Carbon (ASAC) was investigated using the pseudo first-order, pseudo second-order kinetic, Elovich and intraparticles diffusion models. The adsorption isotherms of MB onto ASAC are determined and correlated with common isotherm equations. The smaller *RMSE* value obtained for the Langmuir model indicates the better curve-fitting and the monolayer adsorption capacity of MB is found to be 46.03 mg/g at 25 °C and 88.50 mg/g at 70 °C and pH 10. The evaluation of thermodynamics parameters such as the negative free energy ΔG^{o} (+2.70025 to -1.76666 kJ/mol) and positive enthalpy change ΔH^{o} (28.87613 kJ/mol) indicated a spontaneous and endothermic nature of the reaction with chemisorption process. This study in tiny batch gave rise to encouraging results, and we wish to achieve the adsorption tests in column mode under the real conditions applicable to the treatment of industrial effluents. The present investigation showed that ASAC is potentially a useful adsorbent for the heavy metals and dyes.

Keywords: Apricot stone, Methylene blue, Isotherm, Removal, Thermodynamics, Modelling

Introduction

The effluents from the textile, leather, food processing, dyeing, cosmetics, paper, and dye manufacturing industries are important sources of pollution [1]. Many dyes and their break down products may be toxic for living organisms, particularly methylene blue (MB) [2]. Therefore, the discoloration of dyes is an important aspect of the wastewater treatment before their discharge in the aquatic environment. It is difficult to remove the dyes from such effluents, because they are not readily degradable and are not removed generally from the sewage by conventional techniques. The electrochemical treatment, coagulation and flocculation, chemical oxidation, liquid-liquid extraction, and adsorption were found to be effective for removing organic matter from aqueous solutions in terms of initial cost, simplicity of design, ease of operation, and insensitivity to toxic substances [3]. The synthetic dyes are among the main contaminants in the aquatic medium accounting for about 20 % of the total pollution. They cause several problems beginning by disturbing the eco-system: their presence in water, even at very low concentrations, is highly visible and undesirable. The coloration attenuates considerably the penetration of sunlight into water, retards the photosynthesis, inhibits the growth of aquatic biota, and interferes with gas solubility in water bodies.

In addition, the dyes in water give rise to a chemical oxygen demand, biochemical oxygen demand, and high-suspended solids. Since they are complicated organic compounds that resist to the light, washing, and microbial invasions, they cannot be decomposed easily [4]. Direct discharge of dyes containing effluents may cause the formation of toxic carcinogenic breakdown products. The highest rates of toxicity were found amongst basic and diazo direct dyes [5].

Activated carbon is a versatile adsorbent which has been used widely for the adsorption process, but remains relatively expensive. Consequently, many authors have studied the feasibility of low cost and abundantly available substances that are used for the synthesis of activated carbon. This has prompted a growing research interest in the production of activated carbons from renewable and cheaper precursors which are mainly industrial and agricultural by-products, for the wastewater treatment. However, the activated carbons available in the commerce are relatively expensive and their production and regeneration constitute limiting factors. Hence, many researchers have focused on the search on new low-cost precursors issued from agricultural wastes such as Oil palm biomass [6], date palm [7], olive stones [8], sawdust [9,10], rice husk [11], and apricot stone [12,13]. The remarkable adsorption capacity of activated carbons is due to their well-developed porous

*Corresponding author: moussaiap@gmail.com

structure and pore size distribution, as well as the surface functional groups.

Since Apricot Stone Activated Carbon (ASAC) has exceptional mechanical properties, unique electrical property, highly chemical stability, and large specific surface area, it has attracted a great interest as adsorbent and offers an attractive option for the removal of both organic and inorganic contaminates [14]. In the present work, ASAC is selected to remove methylene blue (MB) from aqueous solution. MB is the most commonly used substance for dyeing cotton, wool, and silk. Although it is not strongly hazardous, it is responsible for several harmful effects where acute exposure to MB causes increased heart rate, nausea, vomiting, shock, cyanosis, jaundice, quadriplegia, and tissue necrosis in humans [15].

The main objective of this research was to evaluate the adsorption aptitude of ASAC for the removal of MB, a model compound for basic dyes. The effects of pH, contact time, initial dye concentration, stirring speed, adsorbent dosage, and temperature on the adsorption capacity were investigated. Moreover, the kinetic and equilibrium models were used to fit the experimental data and the thermodynamic parameters were determined.

Agricultural by-products exist in large amounts and about 20,000 tons of apricot stones are produced annually in Algeria [16]. Over the past, these by-products were used as fuel in rural areas but currently the preparation of activated carbon is considerably encouraged. Since apricot stone is a cheap precursor for the activated carbon source, it is important to evaluate its performance as adsorbent. In previous studies, we have developed adsorbent materials with different properties, to achieve selective applications depending on the molecules to be separated. The advantage of the utilization of an abundant and available residual biomass namely the apricot stone as a raw material for activated carbons gives an additional economical interest to the technical studies.

The apricot stone used in the present study was prepared by both chemical and physical activations and this study was carried out with the aim to optimize the initial dye concentration, pH, particle size, contact time, adsorbent dosage, agitation speed, and temperature. In addition, the equilibrium adsorption data were fitted to various equations to obtain constants related to the adsorption phenomena. Equilibrium and kinetic analyses were conducted to determine the factors controlling the rate of adsorption, the optimization of various parameters in dye recovery and to find out the possibility of using this material as low-cost adsorbent for dye removal. The most significant points of this work are summarized as follows:

- Use of the adsorption technique in batch mode, then switch to continuous mode for the treatment of water contaminated by the textile industry.
- The recovery of a food waste (apricot stone), then recovered in water treatment.
- The preparation of an adsorbent with a high adsorption capacity comparable to commercial coal.
- Low preparation cost.
- Tests for recycling of activated carbon.
- To carry out theoretical simulations in the field of water treatment and design of experiments.
- To show that the activated carbon remains the adsorbent of choice for the removal of organic and mineral pollutants.

Experimental

Materials and Methods

Analytical grade reagents were used in all experiments. Basic dye, MB (99 %) was purchased from Merck Company. The chemical structure and properties of MB are listed in Figure 1 and Table 1. Activated carbon was prepared by a conventional method: carbonization and chemical activation with H_3PO_4 as follows. Apricot stones obtained from

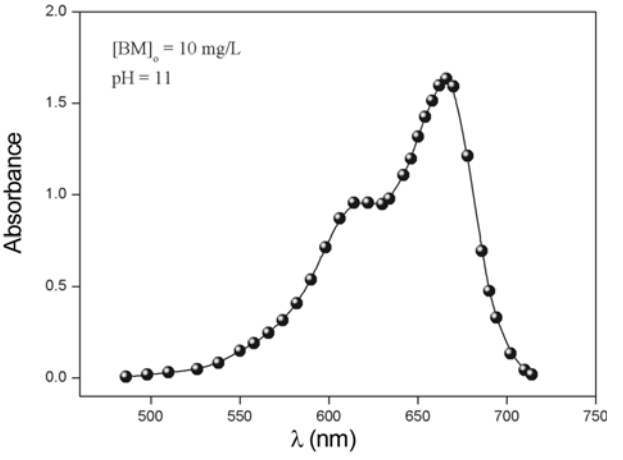

Figure 1. UV-vis spectrum of MB.

Table 1. Chemical and physical properties of basic dye, methylene blue (MB)

Chemical properties	
Molecular formula	$C_{16}H_{18}ClN_3S$
Molecular weight	319.852±0.022 g/mol
Composition (%)	C: 60.08, N:13.00, Cl: 11.08 H: 5.67, S: 10.03
Wave number (λ_{max})	662 nm
Name	Methylene Blue (C.I. Basic Blue 9)
Physical properties	
Melting temperature	180 °C
Solubility in water	50 g/*l* at *T*=20 °C
Solubility in alcohol	10 g/*l* at *T*=20 °C

Boumerdes region (50 km east Algiers), were air-dried, crushed, and screened to obtain two fractions with geometrical mean sizes of 63 and 2.5 mm. 100 g of the selected fraction were impregnated with concentrated H_3PO_4 (85 %) and dried in air. Then, it was activated in a muffle furnace at 250 °C (4 h). The carbonized material was washed with distilled water to remove the free acid until the pH reaches 6.8 and dried at 105 °C. The clean biomass was mechanically ground and sifted to get powders of different particle sizes: from 63 to 2 mm.

Activated Carbon Characterization

Chemical and Physical Analysis of the Prepared (ASAC)

The prepared activated carbon was characterized by selected physical properties (bulk density and surface area), chemical and adsorption properties (point of zero charge: pH_{PZC}).

The elemental analysis was performed by using an elemental analyzer LECO-CHNS 932.

The specific surface area of the activated carbon was determined by the BET-technique, as a sorption phenomenon of N_2 gas on the adsorbent surface, at 77 K. The measurements were made using a Pore Size Micrometric-9320 equipment. The ash content of the activated carbon was determined by heating at 450 °C for 3 h. The conductivity measurements were carried out with a conductimeter type Erwika. The point of zero charge (pH_{PZC}) of ASAC was determined by using potassium nitrate. 20 m*l* of a KNO_3 solution (0.01 M) was placed in different closed conical flasks. The pH of each solution in flask has been adjusted between 2 and 14 by adding solutions of HCl (0.1 M) or NaOH (0.1 M). Then, 0.1 g of ASAC was added and the final pH was measured after 24 h under agitation at room temperature. pH_{PZC} is the point where the curve of final pH versus initial pH crosses the line: final pH=initial pH.

Structural Properties Measurements

The infrared analysis of the prepared ASAC was performed with an IR spectrophotometer of FT Bomen-Michelson type. The IR spectrum was obtained using a KBr disc method. The mixture obtained by grinding 2 mg of the ASAC sample with 98 mg of spectroscopic KBr was pressed into a small disc (∅=1 cm, in thickness of 2 mm). The X-ray diffraction patterns of the native apricot stone (NAS) and ASAC were obtained with a Philips X-ray diffractometer (PW 1890 model).

Batch Mode Adsorption Studies

The effects of the adsorbent dosage (1-10 g/*l*), agitation speed (100-1200 rpm), initial MB concentration (4-15 mg/*l*), pH (2-14), and temperature (298-338 K) on the adsorptive removal of MB were studied in a batch mode of operation for a variable specific period of contact time (0-60 min). The MB solutions were prepared by dissolving the accurate amount of MB (99 %) in distilled water, used as a stock solution and diluted to the required initial concentration and pH is adjusted with HCl or NaOH (0.1 mol/*l*). For the kinetic studies, desired quantities of ASAC were contacted with 10 m*l* of MB solutions in Erlenmeyer flasks. Then, the flasks were placed on a rotary shaker at 300 rpm and the samples were taken at regular time intervals and centrifuged at 3000 rpm for 10 min. The MB content in the supernatant was analyzed on a Perkin Elmer UV-visible spectrophotometer model 550S at (λ_{max}=662 nm). The amount of MB ions adsorbed by activated carbon q_t at time t (mg/g) is calculated by using the following equation (1):

$$q_t = \frac{(C_0 - C_t) \cdot V}{m} \quad (1)$$

where C_0 is the initial MB concentration and C_t the MB concentrations (mg/*l*) at time t, V the volume of solution (*l*), and m the mass of the activated carbon (g). Due to the inherent bias resulting from linearization of the isotherm models, the non-linear regression Root Mean Square Error (*RMSE*) equation (2), the Sum of Error Squares (*SSE*) equation (3), and Chi-squares (χ^2) equation (4) test were employed as criterion for the quality of fitting [14],

$$RMSE = \sqrt{\frac{1}{N-2} \cdot \sum_1^N (q_{e,exp} - q_{e,cal})^2} \quad (2)$$

$$SSE = \frac{1}{N} \sum_{N=1}^{\infty} (q_{e,exp} - q_{e,cal})^2 \quad (3)$$

$$\chi^2 = \sum_1^N \frac{(q_{e,exp} - q_{e,cal})^2}{q_{e,cal}} \quad (4)$$

where $q_{e,exp}$ (mg/g) is the experimental value of uptake, $q_{e,cal}$ the calculated value of uptake using a model (mg/g), and N the number of observations in the experiment (the number of data points). The smaller *RMSE* value indicates the better curve fitting [1,12,14].

Results and Discussion

Structural Properties of ASAC

The physical and chemical properties of ASAC and the elementary analysis are summarized in Table 2. The FTIR spectrum of ASAC is shown in Figure 2. The spectrum displays a number of absorption peaks, indicating the presence of many functional groups in the adsorbent. The band in the region (3122-3680 cm^{-1}) is related to hydroxyl (-OH) groups (intra- and intermolecular hydrogen bonded OH). The bands at 2929 and 1508 cm^{-1} suggest the presence of ($-CH_2$) groups (symmetric and asymmetric) while the band in the region (1600-1665 cm^{-1}) suggests the presence of -C=C- group. The peak at 1732 cm^{-1} is assigned to C=O bond in the carboxylic groups. These results clearly indicate that the functional groups including carboxylic and hydroxyl groups contribute to the adsorption acid dye ions. One can conclude from the XRD patterns of NAS and ASAC show

no definite XRD peaks, suggesting that ASAC is mostly amorphous.

Table 2. Chemical and physical properties of ASAC

Elemental analysis of ASAC (%)	C: 48.45, H: 6.03, N: 0.44 O: 45.08
pH_{PZC}	7.05±0.10
Surface area (m^2/g)	88.05±1.03
Average pore diameter (Å)	176.32±0.25
Average pore volume (ml/g)	0.2641± 0.003
Conductivity (μS/cm)	112.0±2
Humidity (%)	1.48±0.16
The rate of ash (%)	1.68±0.02
The percentage of organic matter (%)	98.32±0.11

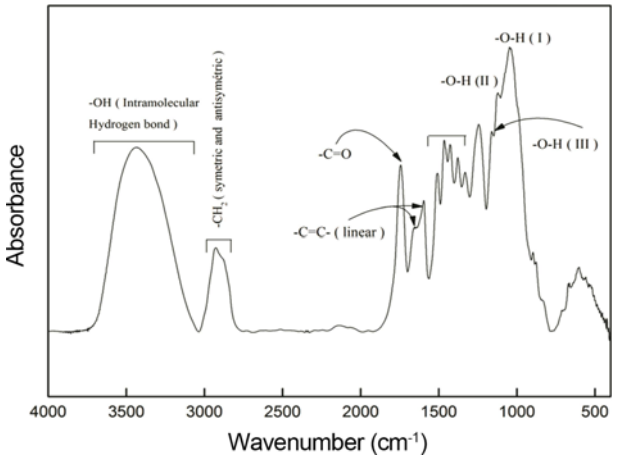

Figure 2. FTIR spectrum of ASAC.

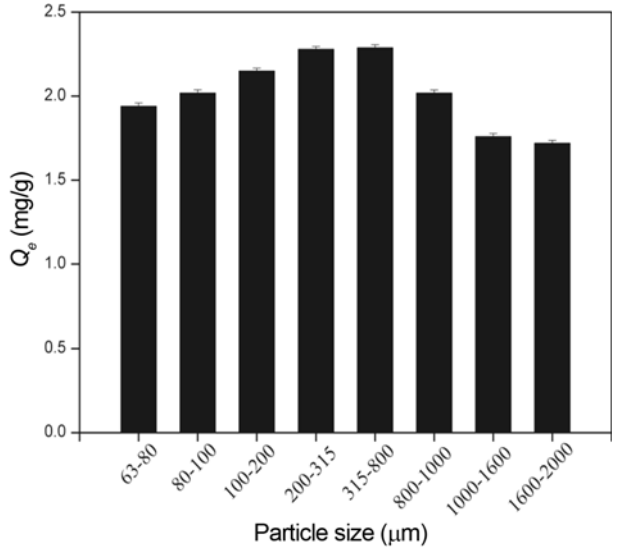

Figure 3. Effect of particle size on the MB adsorption efficiency (T: 25 °C, C_0: 10 mg/*l*, contact time: 45 min, stirring speed: 300 rpm, pH: 8.33, and adsorbent dose: 1 g/*l*).

Effects of Analytical Parameters

Effect of ASAC Size

In the first stage of batch adsorption experiments, the effect of particle sizes on the acid dye adsorption by ASAC is examined. Significant variations in the uptake capacity and removal efficiency are observed at different particles sizes, indicating that the best performance is obtained with lower particle sizes (315-800 μm). In general, smaller particles provide large surface areas, resulting in high MB uptake capacity and removal efficiency. The particle size range (315-800 μm) is subsequently used in all adsorption experiments (Figure 3).

Effect of pH

pH is a crucial parameter in the adsorption process. pH_{PZC} was used to determine the pH at which the net adsorbent surface charge is zero. It is obvious that the percentage of elimination of MB increases with the increase of the pH of the medium (Figure 4). The effect of pH on the adsorption by ASAC can be explained on the basis of pH_{PZC}, for which the adsorbent surface is neutral. The surface charge of the adsorbent is positive when the medium pH is under pH_{PZC} and negative for higher pH than pH_{PZC} of ASAC is 7.05.

This behavior may be due to the fact that the ASAC surface is negatively charged at pH > pH_{PZC}, which favors the adsorption of cationic dyes MB. Conversely, for pH values < pH_{PZC}, the surface of ASAC is positive, and thus it repels the MB molecules. As pH increases, the number of negatively charged sites increases and improves the MB adsorption by electrostatic attractions. Similar experimental details have been reported by Abbas *et al.* [12].

Effect of Stirring Speed

Figure 5 presents the effect of the stirring speed on the MB adsorption onto ASAC. The maximum uptake was obtained

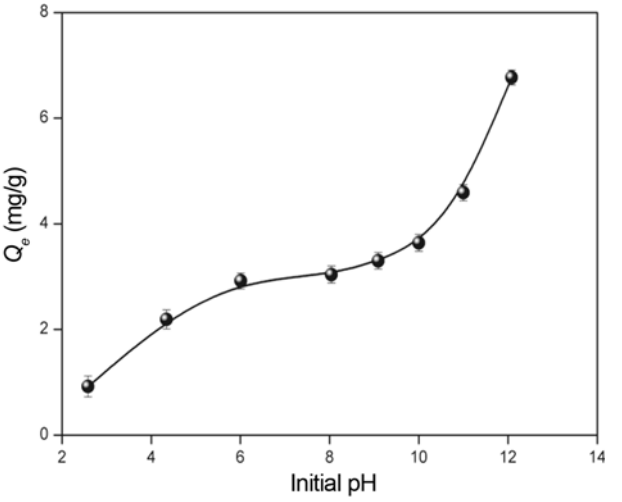

Figure 4. Effect of pH on the MB adsorption efficiency (T: 25 °C, C_0: 10 mg/*l*, contact time: 45 min, stirring speed: 300 rpm, adsorbent dose: 1 g/*l*, and particle size: 315-800 μm).

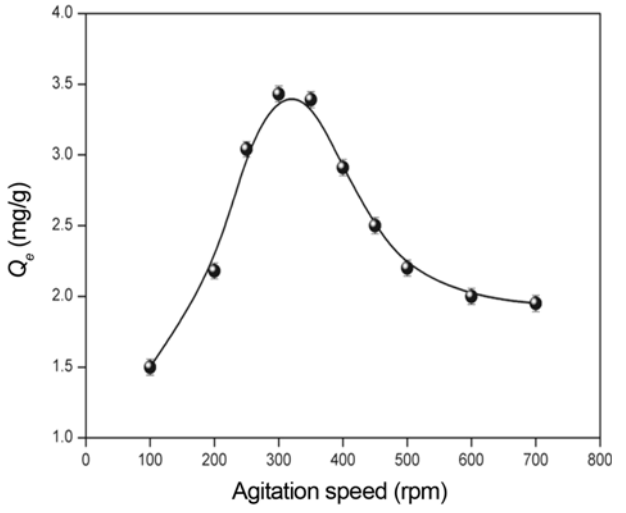

Figure 5. Effect of stirring speed on the MB dye adsorption capacity (*T*: 25 °C, C_0: 10 mg/*l*, pH: 10, adsorbent dose: 1 g/*l*, and particle size: 315-800 μm).

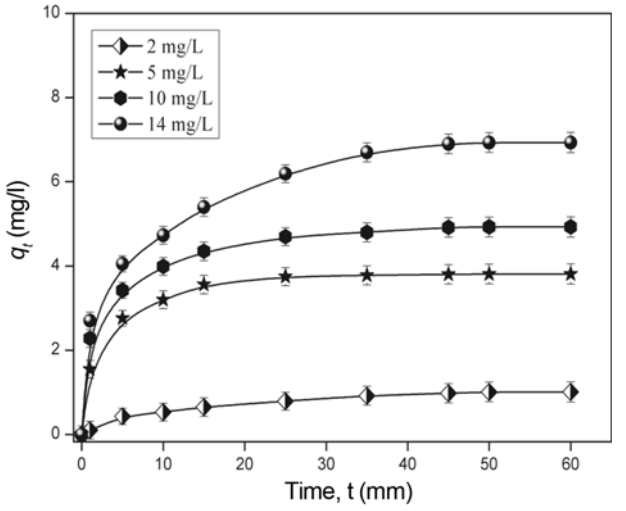

Figure 6. Effect of the contact time on the adsorption of MB onto ASAC for different initial concentrations (*T*: 25 °C, pH: 10, contact time: 60 min, stirring speed: 300 rpm, absorbent dose: 1 g/*l*, and particle size: 315-800 μm).

for a speed of 300 rpm. Such moderate speed gives a good homogeneity for the mixture suspension and precludes the vertex phenomenon.

Effects of Contact Time and Initial Concentration

The adsorption capacity of MB increases with time and reaches a maximum after 40 min and thereafter tends to a constant value, indicating that no more MB molecules are further adsorbed. The equilibrium time is found to be 45 min. The initial MB concentration (2-14 mg/*l*) leads to increased adsorbed amount from 1.4 to 7.51 mg/g (Figure 6). This may be attributed to an increase of the driving force due to the concentrations gradient with increasing the initial dye concentration in order to overcome the mass transfer resistance of MB molecules between the aqueous and solid phases.

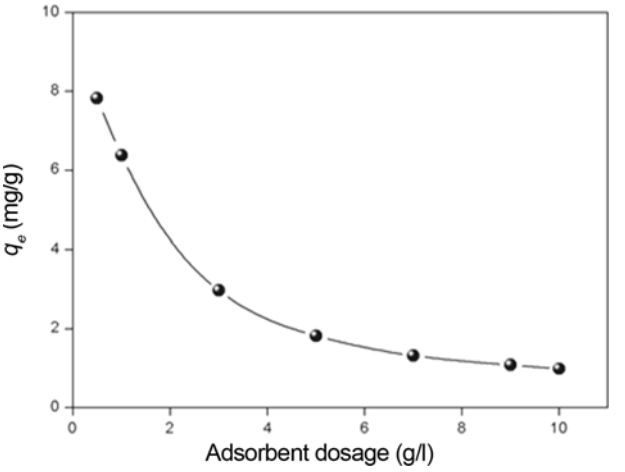

Figure 7. Effect of adsorbent dosage on the MB dye adsorption capacity (*T*: 25 °C, C_0: 10 mg/*l*, pH: 10, stirring speed: 300 rpm, and particle size: 315-800 μm).

Effect of Adsorbent Dose

For the first stage of batch adsorption experiments on ASAC, the effect of adsorbent dosage on the acid dye adsorption is examined. Significant variations in the uptake capacity and removal efficiency observed at different adsorbent dosages (1-10 g/*l*) indicate that the best performance is obtained with a dosage of 1 g/*l* (Figure 7). This result was expected because the removal efficiency-generally increases by more mass available and larger contact surface offered to the adsorption. Moreover, higher dose of adsorbent in the solution, greater availability of exchangeable sites for the ions, i.e. more active sites are available for binding of MB molecules.

Adsorption Isotherms

The shape of the isotherms is the first experimental tool to diagnose the nature of a specific adsorption phenomenon. The isotherms have been classified in four main groups [17]: L, S, H, and C. The isotherms of ASAC at two different temperatures (25 °C and 70 °C) display L type curve (Figure 8(a) and 8(b)). The initial part of the L curve indicates a small interaction between the basic dye and the carrier at low concentrations. However, as the concentration in the liquid phase increases, the adsorption occurs more readily. This behavior is due to a synergistic effect, with the adsorbed molecules facilitating the adsorption of additional molecules as a result of attractive interaction adsorbate-adsorbate. Equilibrium isotherm equations are used to describe the experimental adsorption data. The equation parameters and underlying thermodynamic assumptions of these models often provide insights on both the sorption mechanism and

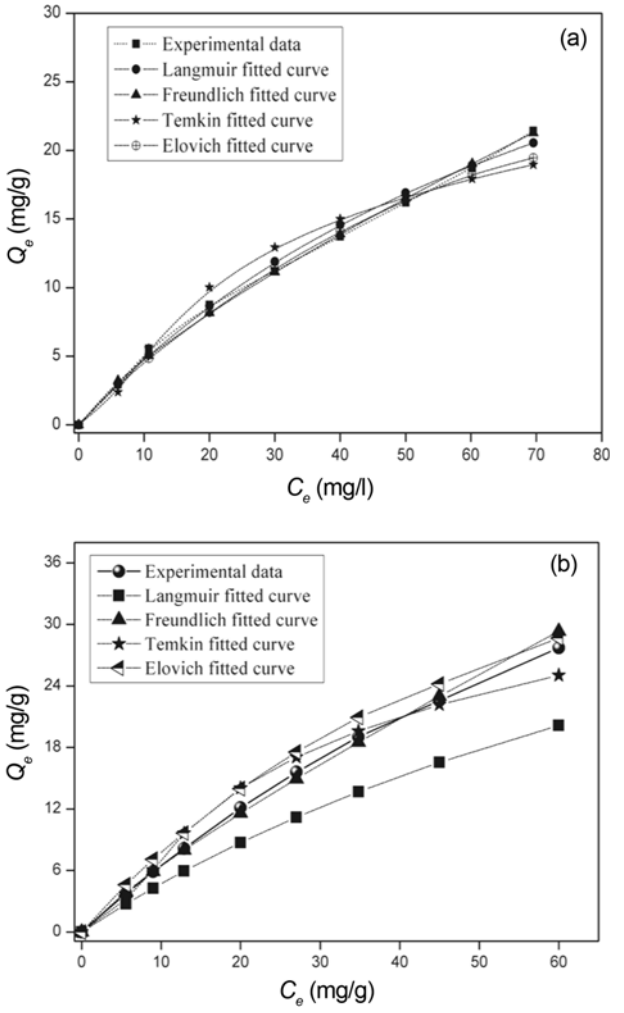

Figure 8. Adsorption isotherm of MB by ASAC at (a) temperature 25 °C and (b) temperature 70 °C.

surface properties and affinity of the adsorbent. The Langmuir equation [18] is widely applied and is represented by the linear form (equation (5)):

$$\frac{1}{q_e} = \frac{1}{q_{\max}} + \frac{1}{q_{\max} \cdot K_L \cdot C_e} \tag{5}$$

where C_e is the equilibrium concentration (mg/*l*), $q_{\max}$ the monolayer adsorption capacity (mg/g), and K_L the constant related to the free adsorption energy (Langmuir constant, *l*/mg). Therefore, the plot of $1/q_e$ versus $1/C_e$ (Figure 9) enables the determination of the constant K_L and $q_{\max}$. The applicability to the adsorption study is compared by evaluating the statistic *RMSE* values. The smaller *RMSE* values obtained at 25 °C for the models indicate a better fitting. The essential features of the Langmuir isotherm can be expressed in terms of dimensionless constant called separation factor, defined by the following equation (6) [19].

$$R_L = \frac{1}{1 + K_L \cdot C_0} \tag{6}$$

where C_0 is the initial concentration of the adsorbate in solution. The R_L indicates the type of isotherm: irreversible (R_L=0), favorable (0<R_L<1), linear (R_L=1), or unfavorable (R_L>1). The R_L values (< 1) confirm that the MB adsorption is favored in both cases as well as the applicability of Langmuir isotherm.

The Freundlich isotherm can be applied to nonideal adsorption on heterogeneous surfaces as well as multilayer sorption; is expressed by the following equations (7) [20].

$$\ln q_e = \ln K_F + \frac{1}{n} \cdot \ln C_e \tag{7}$$

where the constant K_F indicates the adsorption capacity of the adsorbent (*l*/g) and *n* is an empirical constant related to the magnitude of the adsorption driving force. Therefore, the

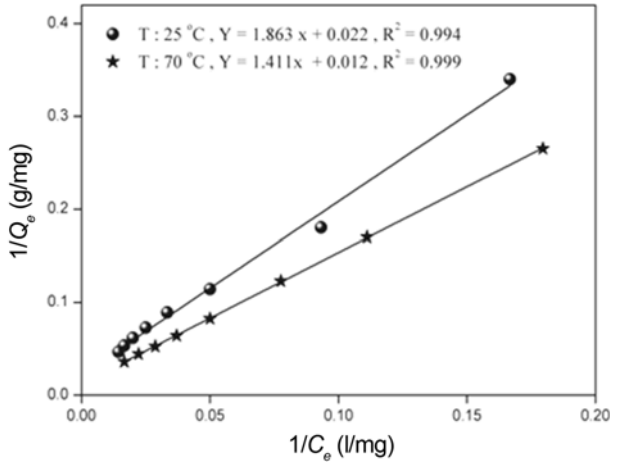

Figure 9. Langmuir isotherms for the adsorption of MB ions onto ASAC.

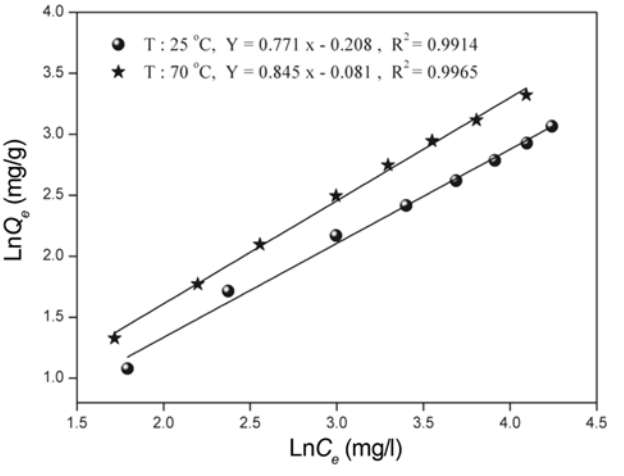

Figure 10. Freundlich isotherms for the adsorption of MB ions onto ASAC.

plot of $\ln q_e$ versus $\ln C_e$ (Figure 10) enables the determination of the constant K_F and exponent n.

The Temkin isotherm describes the behavior of adsorption systems on heterogeneous surfaces, and it has generally been applied in the following form equation (8) [21].

$$q_e = \frac{RT}{b} \cdot \ln AC_e = B \cdot \ln A + B \cdot \ln C_e \quad (8)$$

The adsorption data can be analyzed according to equation (8). Therefore, the plot of q_e versus $\ln C_e$ permits to determine the constants A and B.

The Elovich isotherm [22] is based on the principle of the kinetic assumes that the number of adsorption sites increases exponentially with the adsorption, which implies a multilayer adsorption described by equation (9).

$$\ln\frac{q_e}{C_e} = \ln(q_{\max} \cdot K_E) - \frac{q_e}{q_m} \quad (9)$$

where K_E (l/mg) is the Elovich constant at equilibrium, $q_{\max}$ (mg/g) the maximum adsorption capacity, q_e (mg/g) the adsorption capacity at equilibrium, and C_e (g/l) the concentration of the adsorbate at equilibrium (Figure 11). If the adsorption is described by the equation of Elovich, the equilibrium constant and maximum capacity can be calculated from the plot of $\ln\frac{q_e}{C_e}$ versus q_e. The theoretical parameters of adsorption isotherms along with the regression coefficients, *RMSE*, *SSE*, and are listed in Table 3. The Freundlich isotherm model exhibits the higher *RMSE*, χ^2, and *SSE* values.

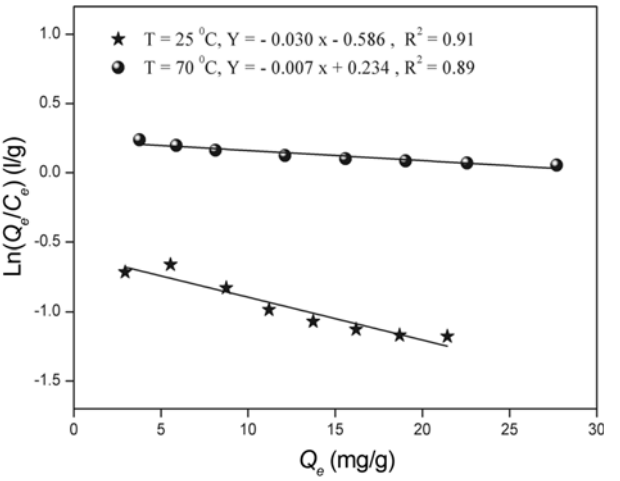

Figure 11. Elovich isotherms for the adsorption of MB ions onto ASAC.

Table 3. Sorption isotherm coefficients of Langmuir, Freundlich, Temkin, and Elovich models

Temperature	T=25 °C		T=70 °C	
Models	Parameters		Parameters	
Langmuir (I)	q_{max}: 45.45 mg/g		q_{max}: 83.33 mg/g	
	K_L: 0.0118 g/mg		K_L: 0.0085 g/mg	
$1/q_{max} = f(1/C_e)$	R^2	0.994	R^2	0.999
	RMSE	0.125	RMSE	0.889
	SSE	0.156	SSE	0.790
	χ^2	0.020	χ^2	0.860
Freundlich	K_F: 0.812 mg/g		K_F: 0.922 mg/g	
	1/n: 0.77		1/n: 0.845	
$\ln q_{max} = f(\ln C_e)$	R^2	0.991	R^2	0.999
	RMSE	0.070	RMSE	0.496
	SSE	0.005	SSE	0.246
	χ^2	0.021	χ^2	0.028
Elovich	q_{max}: 33.30 mg/g		q_{max}: 142.8 mg/g	
	K_E: 0.016 g/mg		K_E: 0.0088 g/mg	
$\ln(q_{max}/C_e) = f(q_e)$	R^2	0.584	R^2	0.89
	RMSE	0.213	RMSE	0.227
	SSE	0.046	SSE	0.051
	χ^2	0.072	χ^2	0.073
Temkin	K_E: 0.202 l/mg		K_E: 0.2028 l/mg	
	β_T: 7.18		β_T: 10.028	
	Δq_{max}: 15.538 kJ/mol		Δq_{max}: 25.167 kJ/mol	
	β_T: $RTq_{max}/\Delta q$		β_T: $RTq_{max}/\Delta q$	
$q_{max} = f(\ln C_e)$	R^2	0.937	R^2	0.948
	RMSE	0.294	RMSE	0.357
	SSE	0.087	SSE	0.127
	χ^2	0.591	χ^2	1.835

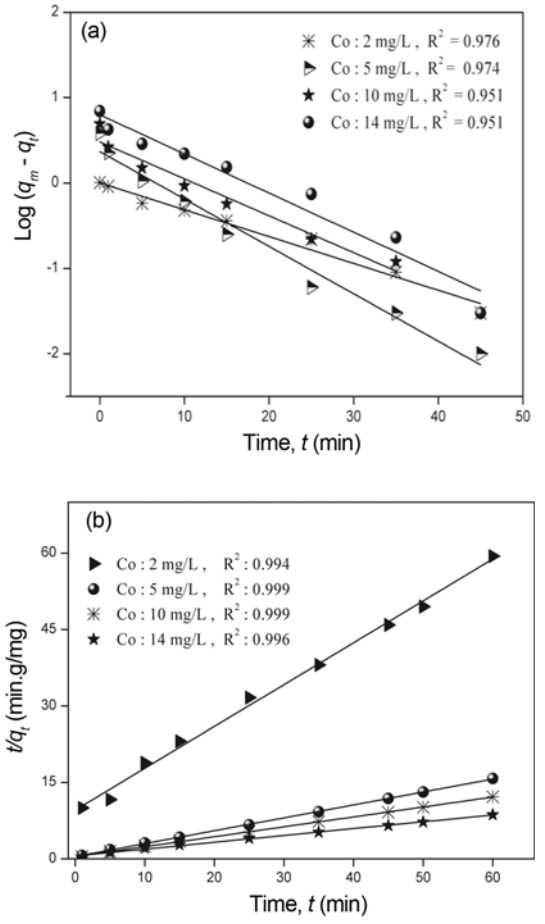

Figure 12. (a) Pseudo first order kinetic for the adsorption of MB onto ASAC (pH 10, particle size: 315-800 μm, adsorbent dose: 1 g/*l*, stirring speed: 300 rpm, *T*: 25 °C, and contact time: 45 min) and (b) Pseudo second order kinetic for the adsorption of MB onto ASAC (pH 10, particle size: 315-800 μm, adsorbent dose: 1 g/*l*, stirring speed: 300 rpm, *T*: 25 °C, and contact time: 45 min).

Adsorption Kinetics

The kinetic study describes the uptake rate of adsorbate and controls the residual time of the whole adsorption process. Two models namely the pseudo first order and pseudo second-order (Figure 12(a) and (b)) are selected in this study to describe the adsorption.

The pseudo first order equation [23] is given in equation (10):

$$\log(q_e - q_t) = \log q_e - \frac{K_1}{2.303} \cdot t \tag{10}$$

The pseudo second order model [24] is expressed by the equation (11):

$$\frac{t}{q_t} = \frac{1}{K_2 \cdot q_e^2} + \frac{1}{q_e} \cdot t \tag{11}$$

where q_t (mg/g) is the amount of metal adsorbed on the adsorbent at various times t (min), K_1 the rate constant of the pseudo-first order kinetic (min^{-1}), and K_2 the rate constant of the pseudo-second order kinetic (g/mg/min).

For the pseudo-first order kinetic, the experimental data deviate greatly from linearity. This was evidenced by the low q_e and determination coefficient R^2 values. Therefore, the pseudo-first order model is inapplicable to this system. The determination coefficient and $q_{e,cal}$ of the pseudo-second order kinetic model are in good agreement with the experimental results (Table 4). The Elovich kinetic model is given by equation (12).

$$q_t = (1/\beta) \cdot \ln(\alpha \cdot \beta) + (1/\beta) \cdot \ln t \tag{12}$$

where α (mg/g/min) is initial adsorption rate, β (mg/g) is constant related to the surface and activation energy of chemisortions, and t (s) is the time.

Table 4. Kinetic parameters for adsorption of MB ions onto ASAC

	Pseudo	2nd order				Pseudo	1st order		
C_0 (mg/*l*)	$q_{e,exp}$ (mg/g)	$q_{e,cal}$ (mg/g)	R^2	$\Delta q/q$ (%)	K_2 (g/mg/min)	$q_{e,cal}$ (mg/g)	R^2	$\Delta q/q$ (%)	K_1 (min^{-1})
2	1.01	1.22	0.994	17.07	0.0714	1.002	0.977	0.79	1.22
5	3.81	3.95	0.999	3.5	0.1425	2.333	0.974	38.76	3.95
10	4.93	5.15	0.999	4.3	0.0856	3.029	0.954	38.40	5.15
14	6.93	7.15	0.996	6.8	0.3191	6.292	0.953	9.235	7.15
		Elovich					Diffusion		
C_0 (mg/*l*)	R^2	β (g/mg)	α (mg/g/min)	C_0 (mg/*l*)	K_{in} (mg/g/min$^{1/2}$)	R^2	C (min$^{1/2}$)	D (cm^2/s)	
2	0.983	4.274	0.298	2	0.0825	0.86	0.4066	0.52×10^{-7}	
5	0.931	1.808	14.03	5	0.0231	0.90	3.6400		
10	0.981	1.488	22.99	10	0.0918	0.86	4.2500		
14	0.979	0.88	9.814	14	0.2717	0.77	4.9600		

$\Delta q/q$ (%): Relative error on the maximum adsorption quantity, D: diffusion coefficient , $D = 0.03\ Ø^2/t_{1/2}$, Ø: particule size (cm), $t_{1/2}$: half equilibrium time (s).

Intraparticle Diffusion Study

An empirically functional relationship common to most adsorption process is that q_t varies proportionally with $t^{1/2}$, the Weber-Morris plot (q_t versus $t^{1/2}$) [25]:

$$q_t = K_{in}t^{1/2} + C \quad (13)$$

The diffusion coefficient is calculated by the following equation.

$$D = 0.03Ø^2/t_{1/2} \quad (14)$$

where K_{in} is the intraparticle diffusion rate constant. Values of intercept C gives an idea about the thickness of the boundary layer. Ø (cm) is particule size and $t_{1/2}$ (s) is half of the equilibrium time. This is attributed to the instantaneous utilization of the most readily available adsorbing sites on the adsorbent surface. The values of K_{in} and C are obtained from the slope while the intercept of linear plots and the constant of the modified Freundlich and Elovich models are listed in Table 4. The adsorption mechanisms and the kinetics can be described according to several models, which can predict the breakthrough curves at different times and accuracies. However, there are not clear criteria to estimate which is the most convenient for a given case, and a lot of concerns must be considered: the mass transfer resistances involved, relation type between the adsorbed amount and the diffusion coefficients, definitive equilibrium equation, and description level as well as mathematical complexity of the model. It is well known that a well realized batch experiment should give valuable data to estimate the diffusion coefficients. Usually, in the real conditions, the mass transport resistance inside the solid is very much higher than through the external fluid film on the solid particles.

Effect of Temperature

The effect of temperature shows that the adsorption capacity of ASAC decreases from 2 to 7.33 mg/g with increasing temperature (295 to 323 K), indicating that the adsorption is disfavored at high temperature. The thermodynamic parameters i.e. the free energy (ΔG^o), enthalpy (ΔH^o), and entropy (ΔS^o) are determined from the following equations (15)-(17) [26]:

$$\Delta G^o = -RT \ln K_0 \quad (15)$$

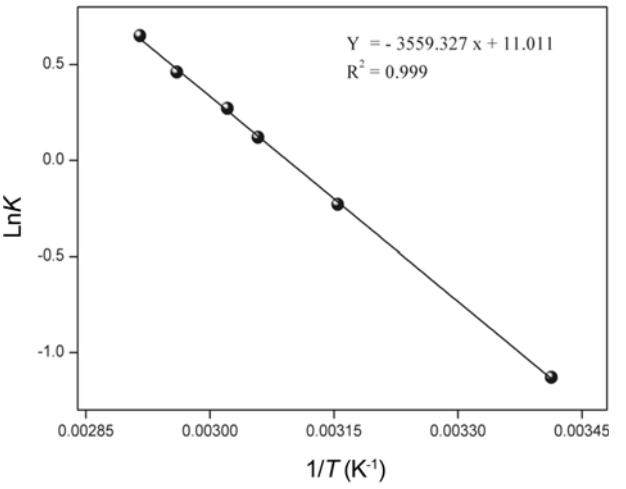

Figure 13. Thermodynamic parameters, enthalpy and entropy for the adsorption of MB ions onto ASAC.

$$\Delta G^o = \Delta H^o - T\Delta S^o \quad (16)$$

$$\ln K = -\frac{\Delta H^o}{RT} + \frac{\Delta S^o}{R} \quad (17)$$

The thermodynamic equilibrium constant K for the sorption was determined [27,28], by plotting q_e/C_e versus C_e and extrapolating to zero q_e. ΔH^o and ΔS^o obtained from the slope and intercept of Van't Hoff plots of ln K versus $1/T$ (Figure 13) and the ΔG^o values at various temperatures are summarized in Table 5.

Some solvents have been tested for regeneration and acetic acid has been shown to be effective in recovering the adsorbent from other solvents.

Performance of the Prepared ASAC

In order to have an idea about the efficiency of the prepared ASAC, a comparison of basic dye adsorption of this work and other relevant studies is reported in Table 6. The adsorption capacity (q_{max}) is the parameter used for the comparison. One can conclude that q_{max} agrees with those of most previous works, suggesting that MB could be easily adsorbed on ASAC prepared in this work. This indicates that the apricot stone, very abundant in Algeria, is a cheap and effective adsorbent for the MB. ASAC is promising adsorbent for metals and basic dyes owing to pH_{PZC} and our

Table 5. Thermodynamic parameters for the MB adsorption on ASAC

T (K)	$1/T$ (K^{-1})	K	ln K	ΔG^o (kJ/mol)	ΔH^o (kJ/mol)	ΔS^o (J/mol/K)
293	3.4130×10^{-3}	0.336216	-1.09	+2.70025	28.87613	89.33749
317	3.1546×10^{-3}	0.794534	-0.23	+0.55615		
327	3.0581×10^{-3}	1.080042	0.077	-0.33722		
331	3.0210×10^{-3}	1.309964	0.27	-0.69394		
337	3.0210×10^{-3}	1.580739	0.46	-1.2306		
343	2.9673×10^{-3}	1.915541	0.65	-1.76666		

Table 6. Comparison of ASAC performances with precursors from previous studies

Dye	Adsorbent		q_{max} (mg/g)	References
Methylene Blue	Bamboo dust carbon		143.20	[2]
	Ground Palm Kernel coat		277.77	[29]
	Bentonite		40.50	[30]
	Kaolin		30.60	.
	Carbon nano tube	T=290 K	103.62	[31]
		T=300 K	109.31	.
		T=310 K	119.70	.
	Activated carbon (strychnos potatorium seed)		100.00	[32]
	Activated carbon (coconut shell fibers)		19.59	[33]
	Activated carbon (olive stones)		303.0	[34]
	Date pits		80.30	[35]
	Zeolite		53.10	[36]
	Modified Sawdust	T=293 K	115.84	[37]
		T=303 K	119.02	.
		T=313 K	160.28	.
	ASAC	T=298 K	46.03	This study
		T=343 K	88.50	This study

perspective is to achieve the adsorption tests in column mode using industrial effluents. Such results are currently under way and will be reported in the near future.

Conclusion

This study has shown that the activated carbon prepared from apricot stone can be employed as effective adsorbent for the removal of methylene blue from aqueous solution. The Elovich and Langmuir isotherms models provided a better fit of the equilibrium adsorption data. They gave a maximum adsorption capacity of 46.03 mg/g at 25 °C which increased to 88.50 mg/g at 70 °C at pH 10. The pseudo-second order model proved the best description of the kinetic data. The negative value of ΔG^o and positive value of ΔH^o indicate that the adsorption of MB onto ASAC is spontaneous and endothermic over the studied temperatures range.

The positive entropy ΔS^o states clearly that the randomness increases at the solid-solution interface during the MB adsorption, indicating that some structural exchange may occur among the active sites of the adsorbent and ions. The MB adsorption follows a pseudo-second order kinetic, which relies on the assumption that chemisorptions may be the rate-limiting step. In chemisorption, the MB ions are attached to the adsorbent surface by chemical bond and tend to find sites that maximize their coordination number with the surface. The kinetics and thermodynamic data can be further explored for the design of an adsorber for industrial effluents treatment. It was noted during the experiments in the laboratory in batch mode that the adsorbent regenerated after several washings showed a decrease of the adsorption capacity (30 %) can be used again efficiently for subsequent use.

Our perspectives in the upcoming research work are as follows:

1. This study in tiny batch gave rise to encouraging results, and we wish to achieve the adsorption tests in column mode under the conditions applicable to the treatment of industrial effluents and the present investigation showed that (ASAC) is a potentially useful adsorbent for the metals, acid and basic dyes.
2. To test the homogeneous photodegradation of dyes on the TiO_2 combined to ASAC semiconductor is the future objective of this work.

References

1. M. Abbas, A. Cherfi, S. Kaddour, and T. Aksil, *Desalin. Water Treat*., **57**, 15037 (2016).
2. N. Kannan and M. M. Sundaram, *Dyes Pigm.*, **51**, 25 (2001).
3. H. Lata, V. K. Garg, and R. K. Gupta, *Dyes Pigm.*, **74**, 653 (2007).
4. E. E. Bezaldez, N. F. Robaina, and R. J. Cassella, *J. Hazard. Mater*., **159**, 580 (2008).
5. A. Ahmad, S. H. Mohd-Setapar, C. S. Chuong, A. Khatoon, W. A. Wani, and R. Kumar, *RSC Adv*., **5**, 30801 (2015).
6. T. Ahmad, M. Rafatullah, and A. Ghazali, *J. Environ. Sci. Health., Part C*, **29**, 177 (2011).
7. T. Ahmad, M. Danish, M. Rafatullah, A. Ghazali, O. Sulaiman, R. Hashim, M. Nasir, and M. Ibrahim, *Environ. Sci. Pollut. Res.*, **19**, 1464 (2012).
8. A. H. El-Sheikh, A. P. Newman, H. K. Al-Daffaee, S. Phull, and N. Cresswell, *J. Anal. Appl. Pyrolysis*, **71**, 151 (2004).
9. P. K. Malik, *J. Hazard. Mater*., **113**, 81 (2004).
10. Y. Guo, J. Zhao, H. Zhang, S. Yang, J. Qi, Z. Wang, and H. Xu, *Dyes Pigm*., **66**, 123 (2005).
11. A. Ahmad, M. Rafatullah, O. Sulaiman, and M. H. Ibrahim, *J. Hazard. Mater*., **170**, 357 (2009).
12. M. Abbas, S. Kaddour, and M. Trari, *J. Ind. Eng. Chem*., **20**, 745 (2014).
13. Z. Harrache, M. Abbas, T. Aksil, and M. Trari, *Microchem. J*., **144**, 180 (2019).
14. M. Abbas, T. Aksil, and M. Trari, *Desalin. Water Treat*., **125**, 93 (2018).
15. A. Ozer and G. Dursun, *J. Hazard. Mater*., **146**, 262 (2007).
16. Annuaire FAO de la Production, Ed FAO, Rome, Italy, www.fao.org, 2009.
17. C. H. Giles, T. H. Mac Ewan, S. N. Nakhwa, and D. Smith, *J. Chem. Soc*., **10**, 3973 (1960).

18. C. Gerent, V. K. C. Lee, P. Le Clorrek, and G. McKay, *Crit. Rev. Environ. Sci. Technol*., **37**, 41 (2007).
19. G. Crini, H. N. Peindy, F. Gimbert, and C. Robert, *Sep. Purif. Technol.*, **53**, 197 (2007).
20. Y. Bulut and Z. Baysal, *J. Environ. Manage*., **2**, 107 (2006).
21. S. J. Allen and G. Mckay, *J. Colloid Interface Sci*., **280**, 322 (2004).
22. A. Ozcan, E. M. Oncu, and A. S. Ozcan, *Colloids Surf. A*, **277**, 90 (2006).
23. S. Lagergren, *Vetenskapsakademiens Handlingar*, **24**, 1 (1898).
24. Y. S. Ho and G. Mc Kay, *Water Res*., **34**, 735 (2000).
25. T. W. Weber and R. K. Chackravorti, *AIChE J.*, **20**, 228 (1974).
26. Z. Harrache, M. Abbas, T. Aksil, and M. Trari, *Desalin. Water Treat*., **147**, 273 (2019).
27. M. Abbas and M. Trari, *Process Saf. Environ. Prot*., **98**, 424 (2015).
28. T. Aksil, M. Abbas, M. Trari, and S. Benamara, *Microchem. J*., **145**, 35 (2019).
29. N. A. Oladoja, C. O. Aboluwoye, and Y. B. Oladimeji, *Turk. J. Eng. Environ. Sci*., **32**, 303 (2008).
30. B. Benguella and A. Yacouta Nour, *Compte Rendu de Chimie*, **12**, 762 (2009).
31. Z. Shahryari, A. Soltani Goharrizi, and M. Azadi, *Int. J. Water Resour. Environ. Eng*., **2**, 16 (2010).
32. M. Jerald Antony Joseph and N. Xavier, *Int. J. Appl. Biol. Pharm*., **3**, 27 (2012).
33. G. T. Faust, J. C. Hathaway, and G. A. Millot, *Am. Mineral*., **44**, 342 (1959).
34. E. Vousdria, K. Fytianos, and E. Bozani, *Global NEST J*., **4**, 75 (2002).
35. D. Suteu and D. Bilba, *Acta Chem. Slov*., **52**, 73 (2005).
36. R. J. Stephansen and J. B. Sheldo, *Water Res*., **30**, 781 (1996).
37. W. Zou, H. Bai, S. Gao, and K. Li, *Korean J. Chem. Eng*., **30**, 111 (2013).